Stark-ladder resonances in ordered and disordered electrified chains

Ernesto Cota
Laboratorio de Ensenada, Instituto de Física, Universidad Nacional Autónoma de México, Apartado Postal 2681, Ensenada, Baja California, Mexico

Jorge V. José* and Guillermo Monsiváis
Instituto de Física, Universidad Nacional Autónoma de México, Apartado Postal 20-364, 01000 México 20, Distrito Federal, Mexico

(Received 3 October 1986)

The electronic energy spectrum of a one-dimensional chain with periodic and disordered potentials in the presence of a constant electric field F is studied. Under certain conditions the spectrum shows the resonant states predicted by Wannier. These Stark-ladder resonances (SLR) are studied in detail for different potentials, amount of disorder, W, and length of the chains, L. Thermal population effects on the resonances are also considered. The different potentials correspond to rectangles with random widths and different heights, that include the extreme δ-function limit. The Poincaré-map method is used to calculate the reflectivity and transmittivity of the chains. Use is made of different scattering theory criteria to characterize the resonances. For electrons incident on the chain with energies, $E \leq FL$, the electrostatic potential energy produced by the field, Levinson's theorem is used to calculate the density of states from the derivatives of the phase shifts with respect to E. For energies $E \geq FL$, the transmission coefficient T is calculated as a function of E, and the SLR appear as equally spaced maxima of T as E is varied. From resonance and ensemble averages the following results are presented: (i) When L is fixed, there is a minimum value of F above which the resonances are clearly present. (ii) The effect of disorder is to perturb the mean properties of the resonances. The mean separation distance between resonances is affected by disorder, and it grows linearly with W, and the variance grows as well. The half width at half maximum (HWHM) of the resonances grows as W^2. (iii) In the periodic as in the disordered cases, the HWHM goes to zero as $\sim e^{-B(W,V_0)/F}$. (iv) As the temperature τ is varied, the height of the resonances decreases as τ^{-1}. As a function of the height of the potential barriers, V_0, it is found that the results qualitatively remain the same. However, quantitatively the results change, for instance, for fixed E, the HWHM increases as V_0 decreases. Finally, a critical discussion of the results is given to assess the possible experimental observation of these resonances in disordered quasi-one-dimensional devices.

I. INTRODUCTION

The possibility of studying experimentally the transport properties of very small structures that behave like quasi-one-dimensional systems has led to a fruitful cross fertilization between theory and experiment. One of the very interesting possibilities offered by these samples is that of seeing resonant tunneling (RT) in disordered systems. This idea, originally considered by Lifshitz and Kirpichenkov,[1] has been extensively developed by Azbel and collaborators.[2] Several experiments have intended to detect RT in ultrasmall silicon structures.[3] In a recent experiment by Fowler *et al.*, some evidence is given for the appearance of RT in these systems.[4] However, there are a number of questions that remain to be answered with regard to the theoretical explanation of their results. One of the possible difficulties in observing RT is that in one-dimensional disordered systems these resonances have a width that is expected to decrease exponentially with the size of the sample. This comes from the fact that in the infinite size limit the resonances should become bound states and therefore their widths should be zero.

In this paper we study another type of resonances, produced by a constant electric field, that have some advantages over the ones studied by Azbel and collaborators. They have also some experimental disadvantages that we will discuss at the end of the paper. These resonances were first proposed by Wannier in periodic systems, and are known as Stark-ladder resonances (SLR's).[5] The SLR's are the analog of the Landau levels which appear in a system of electrons subjected to an externally applied magnetic field. The SLR's are equally spaced poles of the Green function associated to the Schrödinger operator in the presence of a constant electric field. The separation distance between SLR's is directly proportional to the field strength F. The existence of the SLR's have been controversial for some time, but by now some of their properties in periodic systems at zero temperature seem to be theoretically on firm ground.[6] The experimental conditions to see SLR's are very stringent and, although several experiments have claimed to see the SLR's,[7] there is no convincing evidence supporting these claims.

Recently, there have been a number of papers dealing with the properties of electrons in disordered potentials

subjected to a constant electric field.[8–14] The model considered in these papers is defined by the Schrödinger equation,

$$\left[-\frac{d^2}{dx^2}+V(x)-Fx\right]\Psi(x)=E\Psi(x)\ , \tag{1}$$

where Ψ is the wave function, E is the electronic energy, $F=e\mathscr{E}$ with e the electronic charge and $\mathscr{E}$ the electric field strength. We have taken atomic units with $\hbar^2/2m=1$. In the $F=0$ case with random $V(x)$, it has been rigorously established that in this model all the electronic states are localized with wave functions with an envelope that decays exponentially with distance. The spectrum of the infinite system is pure point, i.e., discrete, and the resistance increases exponentially with the length of the sample.[15] For $F\neq 0$, it has been found that the electric field has a qualitatively dramatic effect in the electronic properties of the model. These changes are strongly dependent on the type of potential V, and a ratio between the electrostatic energy gained by an electron traversing the sample of length L and its incoming energy, i.e., $X=FL/E$,[12] the energy being measured from the top of the ramp potential produced by the electric field.

When $V(x)$ is a set of δ functions located in a periodic lattice, with random strengths and $X<1$, the states are localized and the transmission coefficient T, as a function of the length of the sample L, has essentially an exponential decay. When $X>1$, T has a power-law decay as a function of L, with an exponent that depends on $1/F$. There is a critical field F_c above which the states are extended, however.[10–12] For random potentials of finite height, it was found that the $X\ll 1$ regime is qualitatively similar to that of the δ-function case. Quantitatively, however, the results are different, and depend explicitly on the analytic properties of the potentials. When $X>1$, the transmission coefficient tends to a constant as L tends to infinity.[12] This constant has a nonlinear dependence on F as L becomes infinite. One of the questions addressed in this paper is to which extent the SLR's depend on the type of potential $V(x)$. The goal of this paper is to analyze the properties of SLR's in periodic but mainly in disordered systems. The models considered are defined by Eq. (1) with different forms for the lattice potential $V(x)$. We use different scattering theory criteria to characterize the SLR's, their dependence on disorder and their statistical properties.

The scattering problem can be divided in two parts: when the electron is incident below and when it is incident above the ramp produced by the electric field. In the former case, the reflection coefficient is equal to one and information on the resonances is obtained from the phase shifts of the S matrix, which in this case coincides with the reflectivity coefficient.[16] For energies above the barrier, of more interest experimentally,[17] we calculate the transmission coefficient as a function of energy. For relatively large values of the field, but below the critical fields mentioned above, the SLR's appear as maxima of T. The maxima, although close to one, are not always one. This is clearly related to the fact that T, which is proportional to a product of wave-function amplitudes, in the disordered case as well as in the ordered case with a field, does not have to lead to T equal to one at resonance, as happens in the purely periodic case with $F=0$, since either the disorder or the electric field can produce localization of the wave function (see further discussion below). Further information on the properties of these resonances is obtained from an analysis of the resonance circles. The half width at half maximum (HWHM) of the SLR's, defined in terms of the maxima of T, is analyzed in both cases as functions of F and the amount of disorder. The role of thermal population effects in the independent electron model is considered in the spirit of Ref. 2. We present numerical and heuristic analytic analyses of the effects of temperature on the SLR's. Some of the results on the δ-function potential were announced elsewhere.[18,19] Here details and extensions of those results are given, and a detailed study of other potentials, as well as the thermal population effects on the SLR's are discussed.

The outline of the paper is as follows: In Sec. II we define the models considered in this paper. The Poincaré map for a general potential V is discussed, the explicit algorithm to calculate the reflectivity and transmittivity is given as well as a method to reliably calculate the derivatives of their phases. In Sec. III we consider the zero-temperature properties of the SLR's above and below the ramp, with the approach developed here. In the periodic case explicit comparison is made between the results obtained here and those of Bentosela *et al.*[6] who use a Green function approach to calculate the SLR's for energies below the ramp. The disordered case is considered in Sec. III as well. To obtain statistically significant results we take a double average: one with respect to different resonances in the same sample, and the other one among samples with different random potentials drawn from the same probability law. In Sec. IV we consider, numerically and analytically, the effects of temperature on the SLR's. Finally, in Sec. V a critical discussion of the results is presented with an assessment as to what is needed to see experimentally the SLR's in quasi-one-dimensional systems.

II. METHOD OF CALCULATION

In this section we define the models to be studied. The Poincaré map (PM) for random rectangular potentials in a field is derived. The methods to calculate the reflectivity, transmittivity, and their corresponding phases, together with their derivatives in terms of a simultaneous solution of two PM's, are discussed.

A. Definition of the models

The potential $V(x)$ considered in this paper, has the property that it can be expressed as $V=\sum_n V_n(x)$, and V_n is given by, (see Fig. 1)

$$V_n(x)=\begin{cases} V_0, & \text{if } x\in l_n=b_n, \text{ with } n \text{ even} \\ 0, & \text{if } x\in l_n=a-(b_{n+1}+b_{n-1})/2\ , \end{cases} \tag{2a}$$

with n odd ,

where $l_n=x_{n+1}-x_n$. Thus, b_n with n even is the width

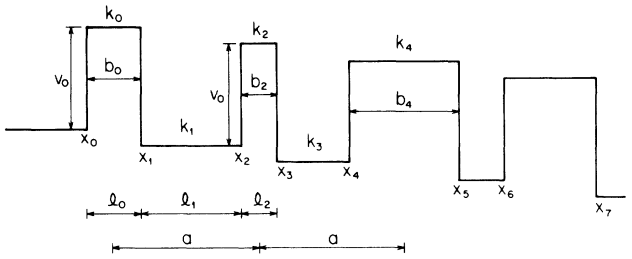

FIG. 1. The random rectangular potential used in the calculations presented in this paper. The variables l_n, K_n, and b_n are defined in Eq. (3).

of the nth barrier and a is the spacing between the centers of the barriers. In the disordered case, b_n is a random variable chosen with a uniform probability law,

$$P(b_n)=\begin{cases}1/W, & \text{if } b_c-W/2<b_n<b_c+W/2\\ 0, & \text{otherwise}\ ,\end{cases} \tag{2b}$$

i.e., the width fluctuates around a fixed value b_c. The interpotential separation a is kept fixed throughout the calculations. This type of potential interpolates between the δ-function case, and the finite potential barrier limit. The δ-function case is obtained in the limit $V_0\to\infty$, $b_n\to 0$ with $V_0 b_n=\beta_n$, finite and fixed. As in previous works,[9–12,16,18–19] the electric potential $-Fx$ is approximated by a ladder with excellent results. The total potential $V(x)$-Fx, is then given as (see Fig. 1)

$$V(x)-Fx=\begin{cases}FL, & \text{if } x<0\\ FL-F\displaystyle\sum_{n=1}^{N} l_n\Theta(x-na)+\sum_n V_n(x)\\ 0 & \text{if } x>L\end{cases} \tag{3}$$

Here $\Theta(x)$ is the usual step function and $Na=L$. Notice that in Eq. (3) the zero of energy is chosen at the bottom of the ramp. There are some calculations for which choosing the zero at the top is more convenient, as will be discussed later on.

B. Poincaré-map approach

The problem of interest here is to calculate the scattering properties of a wave incident upon the potentials present in the sample in the interval $0\le x\le L$. For a wave incident from the right with unit amplitude, there is a reflected and a transmitted wave, which have the expressions,

$$\Psi(x)=\begin{cases}re^{iK_+x}+e^{-iK_+x}, & \text{if } x+\infty\\ te^{-iK_-x}, & \text{if } x\to-\infty\ .\end{cases} \tag{4}$$

In these equations r and t are the reflectivity and transmittivity coefficients, respectively. The wave vectors are defined as $K_\pm=(E-V_\pm)^{1/2}$ where $V_+=0$ and $V_-=FL$. Since there is conservation of probability, r and t satisfy the relation,

$$\frac{K_-}{K_+}|t|^2+|r|^2=1\ . \tag{5}$$

There are two cases which are distinct from the scattering theory point of view: (a) when $0<E<FL$, and (b) when $FL<E$. In case (a) the transmittivity tends to zero as $x\to-\infty$, and the reflection coefficient $R=|r|^2=1$. The S matrix is simply equal to r, and can be written as,

$$S=r=e^{2i\delta(E)}\ , \tag{6}$$

in which $\delta(E)$ corresponds to the phase shift of the reflected wave. An analysis of the behavior of δ as a function of E yields information about the location of the resonances. However, to find the location of the resonances with precision we use Levinson's theorem, which gives the density of states, $n(E)$, simply in terms of the derivative with respect to E of the phase shift,[20]

$$n(E)=2\pi\delta'(E)\ . \tag{7}$$

This is the approach followed here to find the energy spectrum for case (a). An alternative calculational approach, used in the periodic case by Bentosela *et al.*,[6] is to find the poles of the Green function analytically continued to the unphysical sheet.

Case (b) is more interesting from the experimental point of view, and we will concentrate on that case for the most part in this paper. In this case the quantity of experimental interest is the transmission coefficient T. However, it is shown that the derivative with respect to E of the phase of the reflectivity, as well as an analysis of the resonance circles give added information about the properties of these resonances.

To calculate the quantities of interest in case (b), we can use either the transfer-matrix approach, like the one used in Ref. 12, or the PM method introduced for the δ-potential problem in the $F\neq 0$ case in Ref. 10. It turns out, that it is not easy to use the transfer-matrix approach to calculate the derivatives of the phases with respect to E, since it entails the derivative of a product of N 2×2 matrices. The PM method, on the other hand, gives a unified treatment for the calculation of all the quantities of interest in both regimes, since taking a derivative of the PM itself is relatively easy and yields accurate results. Therefore, the PM method was used in the calculations presented in this paper.

To derive the Poincaré map corresponding to Eq. (1), with the potential given in Eq. (3), we proceed as follows: Define the wave-function amplitude at site n as $\Psi_n=\Psi(x=na)$. A PM gives a relation between the wave-functions Ψ_{n-1}, Ψ_{n+1}, and Ψ_n. To find this relation, start by writing the solutions to the Schrödinger equation in the step where the potential is equal to V_n,

$$\Psi(x)=A_n e^{iK_n x}+B_n e^{-iK_n x}=\Psi_n^+(x)+\Psi_n^-(x)\ , \tag{8}$$

where $K_n=(E-V_n)^{1/2}$. For simplicity of notation we have defined the waves to the left Ψ_n^-, and to the right Ψ_n^+ within the nth region. Using the boundary conditions for the continuity of $\Psi(x)$ and the continuity of its deriva-

tive at each lattice site, the following equations result:

$$\Psi_{n+1}=\cos(l_nK_n)\Psi_n+\frac{\sin(l_nK_n)}{K_n}\Psi'_n\ , \tag{9}$$

$$\Psi'_{n+1}=-K_n\sin(l_nK_n)\Psi_n+\cos(l_nK_n)\Psi'_n\ , \tag{10}$$

with $'$ denoting the derivative with respect to x. This set of first-order finite difference equations are equivalent to Hamilton's equations in classical mechanics. Substituting Ψ'_n from Eq. (10) into Eq. (9), we obtain the second-order difference equation,

$$\Psi_{n+1}=\left[\cos(l_nK_n)+\frac{K_{n-1}\sin(l_nK_n)}{K_n\sin(l_{n-1}K_{n-1})}\cos(l_{n-1}K_{n-1})\right]\Psi_n-\left[\frac{K_{n-1}\sin(l_nK_n)}{K_n\sin(l_{n-1}K_{n-1})}\right]\Psi_{n-1}\ . \tag{11}$$

This is the PM studied in this paper. It is a second-order linear finite difference equation, that can be solved given two initial conditions, say Ψ_1 and Ψ_0. In the δ-potential limit, the PM given in Eq. (11) reduces to,

$$\Psi_{n+1}=\left[\cos(aK_n)+\frac{K_{n-1}\sin(aK_n)}{K_n\sin(aK_{n-1})}\cos(aK_{n-1})+\beta_n\frac{\sin(aK_n)}{K_n}\right]\Psi_n-\left[\frac{K_{n-1}\sin(aK_n)}{K_n\sin(aK_{n-1})}\right]\Psi_{n-1}\ , \tag{12}$$

which is the map studied in Ref. 10. When there is no field applied, and $V=V_0$, Eq. (12) reduces to

$$\Psi_{n+1}=\left[\beta_n\frac{\sin(aK_0)}{K_0}+2\cos(aK_0)\right]\Psi_n-\Psi_{n-1}\ , \tag{13}$$

where $K_0=\sqrt{E}$. Equation (13) is the PM derived by Bellisard *et al.*,[21] and contains all the information about the band structure of the periodic Kronig-Penney model. Similarly, Eq. (11) has all the band-structure information contained in Eq. (1), and this fact is essential to understand the properties of an electron in a lattice potential subject to an electric field. In the early studies of (SLR's), a one-band approximation was used, and therefore a number of criticisms to those studies ensued.[22]

By changing the values of V_0 and l_n in Eq. (11), we can go from the extreme δ-potential limit to a finite height rectangular potential. Of course, in this map equation the case of continuous potentials is not included. However, as found in Ref. 12, the localization properties of disordered rectangular and continuous potentials have characteristics that are qualitatively similar, although quantitatively they do depend on the specific analytic properties of the V's.

The reflection and transmission coefficients are obtained from the expressions,

$$R=\left|\frac{\Psi_N^+}{\Psi_N^-}\right|^2,\quad T=\left|\frac{\Psi_{-1}^-}{\Psi_N^-}\right|^2. \tag{14}$$

From the PM given in Eq. (11), it follows that,

$$\Psi_N^-=\frac{e^{3iK_Nl_N}[\Psi_{N+1}-e^{-iK_Nl_N}\Psi_{N+2}]}{e^{2iK_Nl_N}-1}\ . \tag{15}$$

Notice that at the site $n=-1$, the potential is FL, and at $N+1$ it is zero. The calculation of Ψ_N^+ is simply obtained from Ψ_N^- as,

$$\Psi_N^+=\Psi_N-\Psi_N^-\ . \tag{16}$$

From Eqs. (15) and (16), all quantities of interest can be obtained i.e., t and r with their corresponding phases, as well as their absolute values square, T and R. A quantity of possible experimental interest can be defined as a Landauer-type formula,[23]

$$\rho(F,E)=\frac{R}{T}\ , \tag{17}$$

with ρ a generalized dimensionless resistance. For an arbitrary field, the validity of this formula has not been given, but it does reduce to the appropriate Landauer formula in the limit when the F is sufficiently small.[10] For $0<E<FL$, the density of states is calculated from the phase shift as given in Eqs. (6) and (7). Using the fact that $\delta(E)=\frac{1}{2}\mathrm{Im}[\ln(\Psi_N^+/\Psi_N^-)]$, where Im stands for imaginary part, the density of states $n(E)$ is thus obtained from Eq. (7) as

$$n(E)=\frac{1}{4\pi}\mathrm{Im}\left[\frac{\Psi'^+_N}{\Psi_N^+}-\frac{\Psi'^-_N}{\Psi_N^-}\right]. \tag{18}$$

This expression involves Ψ_N and its derivative with respect to E. Since the calculation of Ψ_N is done numerically, the derivative of Ψ_N could be calculated numerically as well. This procedure is, however, inaccurate and time consuming. Instead, $n(E)$ can be obtained from taking the derivative of the PM given in Eq. (11) and iterating the resulting finite difference equation until Ψ'_N is obtained. To iterate this PM, Ψ'_1 and Ψ'_0 have to be given. These are just the derivatives of the initial conditions needed to calculate Ψ_N. Thus, to calculate $n(E)$ reliably it is necessary to iterate two PM's simultaneously. The derivatives of the phase of the reflectivity, named $\theta_r(E)$ above the ramp, also give relevant information about the resonances above the ramp potential, and are calculated in the same way.

III. ZERO-TEMPERATURE RESULTS

In this section the Stark-ladder resonances are studied in detail at zero temperature. In Sec. III A the periodic case is considered for energies above and below the electric field potential. In the δ-function limit, and for $E\leq FL$, a direct comparison of the results obtained from $\delta'(E)$ to results obtained by Bentosela *et al.*[6] is given. The calculations are extended to different potentials above the ramp. It is found that for $E\geq FL$, the derivative of the phase of the reflectivity, $\theta'_r(E)$, has extrema that coincide with the maxima of the transmission coefficient as a func-

tion of E. An interpretation of this result is given in terms of the behavior of the reflectivity in the complex plane and its magnitude. In Sec. III B the disordered case is discussed for $E \leq FL$ and $E \geq FL$. There it is found that, for the same amount of disorder, the SLR's are more stable for $E \geq FL$ than for $E \leq FL$. This is good since the region of experimental interest is $E \geq FL$, and therefore all the statistical analysis of the SLR's in disordered systems is done for $E \geq FL$ when the parameters W, E, F, and L are varied.

A. SLR's in periodic systems

There are different ways to define a resonance, not all giving exactly the same quantitative results.[22] For energies $E \leq FL$, one such definition is given in terms of the poles of the resolvent operator when analytically continued to the unphysical sheet. The SLR's were analyzed from this point of view in Ref. 6. Equivalent ways of defining the resonances is from the poles of the S matrix, or in terms of the rapid changes of the phase shift $\delta(E)$ when changing E. Alternatively, using Levinson's theorem, the maxima of $\delta'(E)$ gives the real part of the resonance and its halfwidth at half maxima (HWHM) is proportional to its imaginary part. For energies above the ramp, the resonances can be defined in terms of the maxima of T or, as is discussed below, by the extrema of $\theta_r'(E)$.

As a test of the scattering method used here to find the SLR, in Fig. 2 we show $\delta'(E)$ for a potential considered in Ref. 6. This potential differs from the one defined in Eq. (3) in that the δ limit has been taken with the δ's located in the middle of each step in the ladder potential, and with the β_n's negative. The parameters used are $N=13$, $a=6$, $L=78$, and $F=0.0125$. The location of the maximum of $\delta'(E)$ corresponds to $E=1.556\,140\,806$, to be compared with the result of Ref. 6, $E=1.556\,140\,828\,094\,9$. The imaginary part of the resonances can be estimated from HWHM/2 of the resonance seen in $\delta'(E)$. The result is $1.820\,62\times10^{-6}$ which, compared with $1.820\,545\times10^{-6}$ from Ref. 6, is not as good as the number obtained for the real part of $\delta'(E)$, but certainly reasonable. The accuracy of the results could be increased by decreasing the size of the energy mesh. However, the point is to show that the scattering approach used here leads to reliable results.

Figure 3(a), shows the results for $\delta'(E)$ for the potential defined in Eq. (3), with $E \leq FL$, for the δ potential. The parameters chosen are $a=1$, $F=0.8$, and $N=100$, with $\beta_n=2$ for all n. In Fig. 3(b), $\delta'(E)$ is shown in a restricted energy range. In this figure there are two sets of SLR resonances that can be distinguished for the energy mesh$=0.005$. It is possible that if we reduce the energy mesh further, subsequent SLR's with larger lifetimes would appear. The average separation distance of the two SLR's for the same energy range is $\langle \Delta E \rangle_1 = 0.800\,096$ and $\langle \Delta E \rangle_2 = 0.800\,008\,78$, respectively. For the former, however, the HWHM is larger than in the latter as can be seen visually and quantitatively giving, i.e., HWHM$=\langle \Gamma \rangle_1 = 0.046\,06$, and HWHM$=\langle \Gamma \rangle_2 = 0.029\,14$.

Next, the case when $E \geq FL$, for the same potential and parameters used in Fig. 3, is considered. Figure 4 presents the results for the transmission coefficient T as a function of energy for three different values of V_0: $V_0=100,20,10$, with $b=0.02,0.1,0.2$, respectively. The first case corresponds to the δ limit, whereas the last one corresponds to the smallest height considered here. The appearance of a SLR is evident in all three cases. In the δ limit, the SLR's are sharper but less so in the shortest height case. The average separation distances between

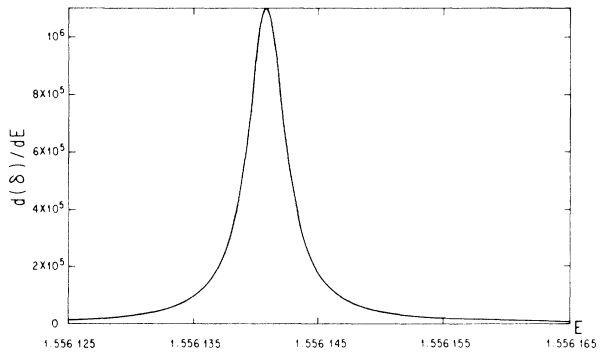

FIG. 2. $\delta'(E)$ vs E for a resonance in a periodic chain with the potential defined in Ref. 6 and parameters $N=13$, $a=6$, $L=78$, and $F=0.0125$.

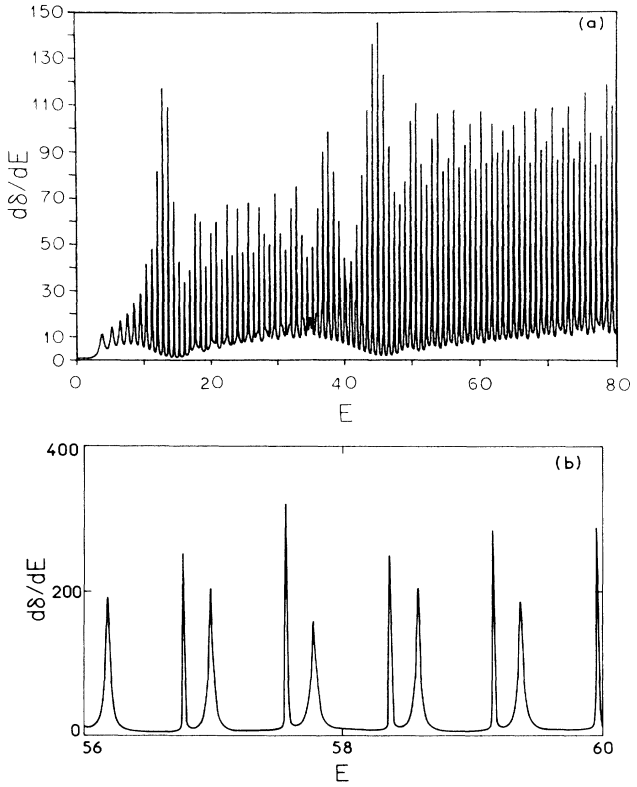

FIG. 3. $\delta'(E)$ for a chain with a periodic δ potential defined in Eq. (3) with $E \leq FL$, $a=1$, $F=0.8$, and $N=100$. In (a) the energy range is from 0 to FL, while in (b) only a restricted energy range is considered.

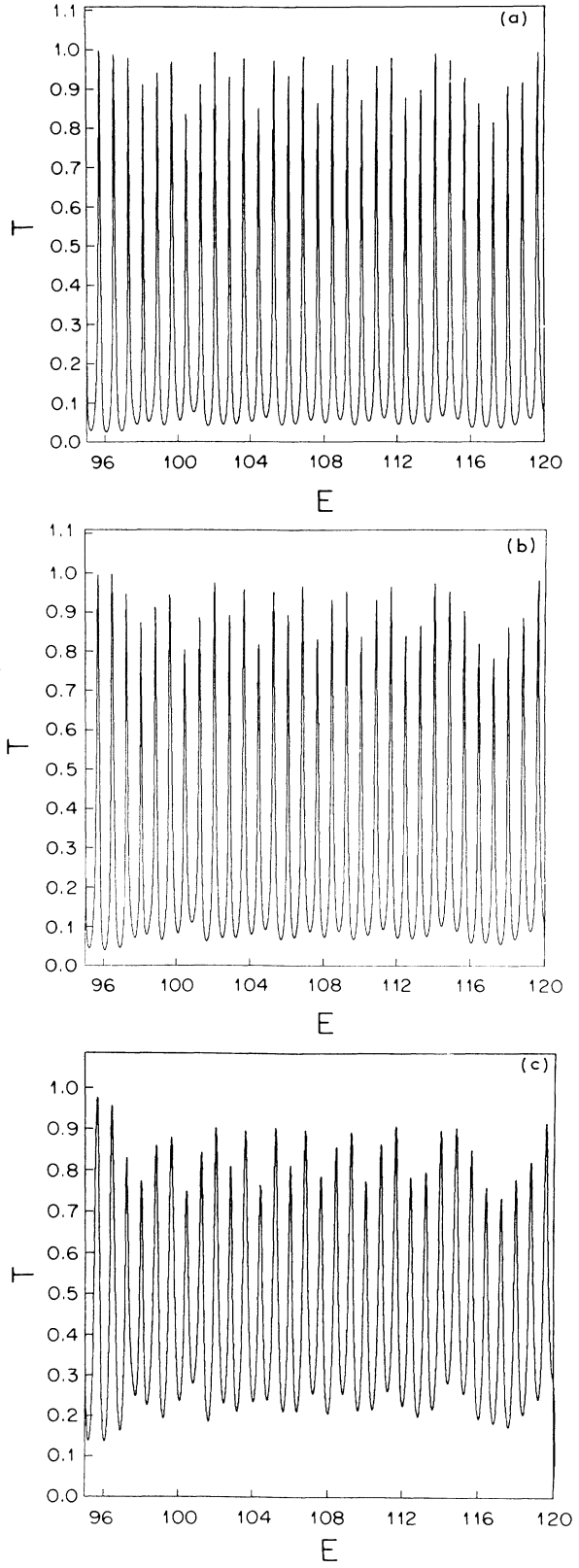

FIG. 4. Transmission coefficient as a function of energy E for three different values of V_0: (a) $V_0=100$, (b) $V_0=20$, and (c) $V_0=10$. All the chain parameters are the same as those in Fig. 3.

TABLE I. Average separation distance between resonances $\langle \Delta E \rangle$ and their corresponding HWHM in the $W=0$ case. The fluctuations about the mean values are also given.

$V_0(\delta)$	$\langle \Delta E \rangle = 0.799\,524\,84$	$\langle \Gamma \rangle = 0.123\,269\,03$
	$\sigma(E) = 0.006\,608\,78$	$\sigma_\Gamma = 0.014\,665\,09$
$V_0(20)$	$\langle \Delta E \rangle = 0.799\,498\,42$	$\langle \Gamma \rangle = 0.157\,589\,81$
	$\sigma(E) = 0.007\,273\,03$	$\sigma_\Gamma = 0.017\,321\,72$
$V_0(10)$	$\langle \Delta E \rangle = 0.799\,380\,16$	$\langle \Gamma \rangle = 0.332\,785\,77$
	$\sigma(E) = 0.008\,578\,47$	$\sigma_\Gamma = 0.028\,035\,18$

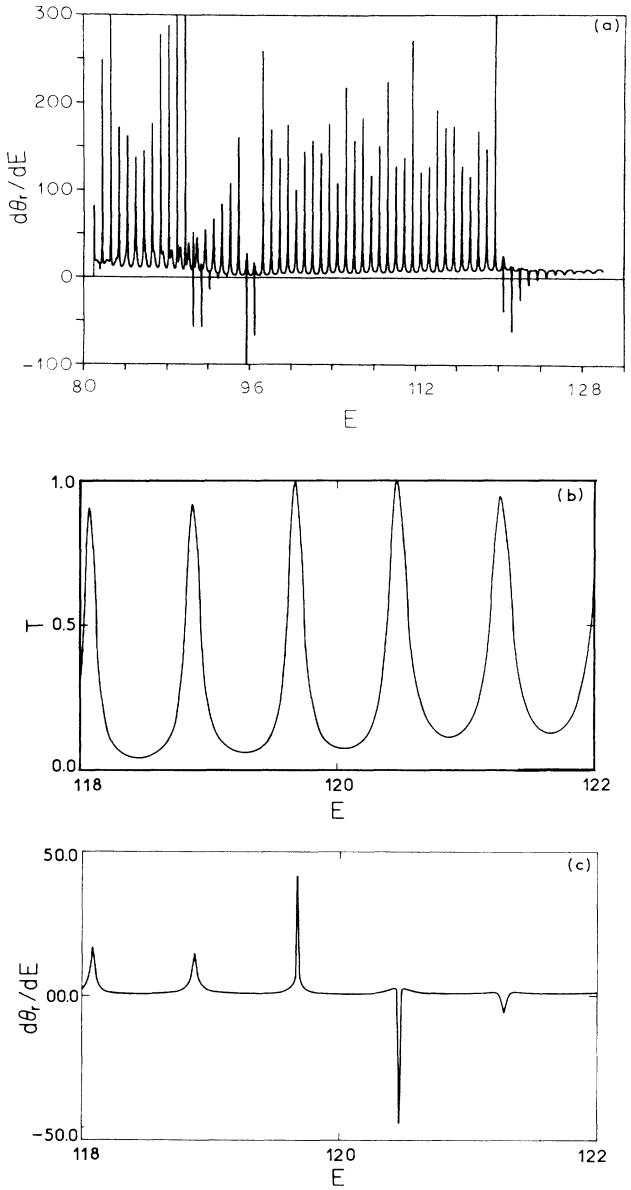

FIG. 5. (a) $\theta_r'(E)$ vs E for the parameter values $a=1$, $F=0.8$, $N=100$, and $\beta=2$. In (b) and (c) there is a restricted energy range of T and $\theta_r'(E)$ for the same parameters as in (a).

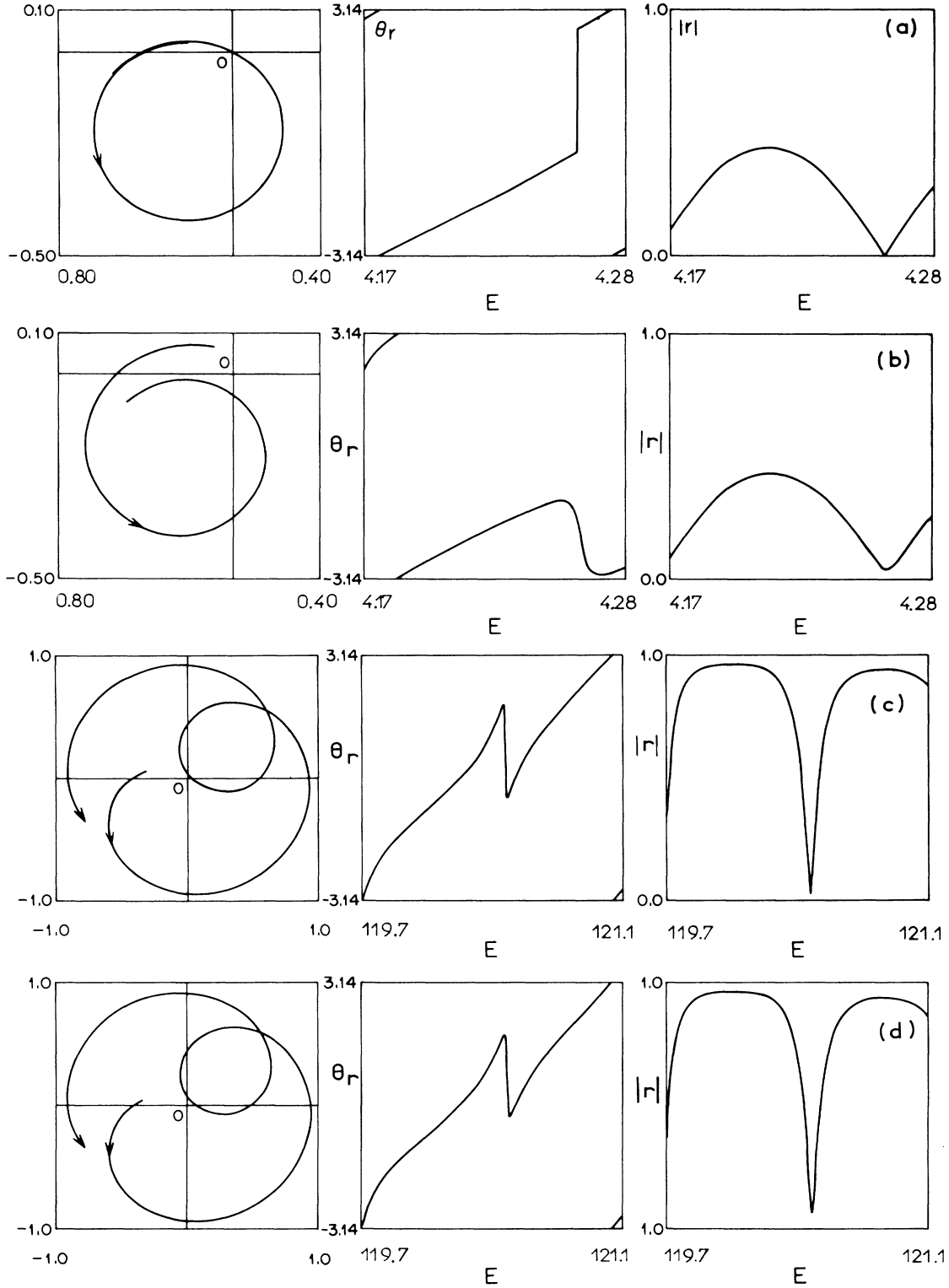

FIG. 6. From left to right, Re(r) vs Im(r), θ_r vs E, and $|r|$ vs E, plotted in an energy range that contains one resonance. In all the figures the parameter values for a and N, are 1 and 100, respectively. (a) presents the results for the periodic case in zero field. The direction of growth in E is shown with an arrow. (b) shows the results when there is disorder with $W=0.06$, and $F=0$. The case shown in the figure corresponds to a resonance with $\theta'(E)<0$. In (c) the periodic case is considered with $F=0.8$. Notice that in this case $\theta'(E)<0$, and the orbits are more complicated. Close to the origin $|r|$ is near zero. In (d), the same parameters as in (c) are used but with disorder of $W=0.2$. Notice that the magnitude of $|r|$ is smaller than in (c) but the structure of the SLR remains stable.

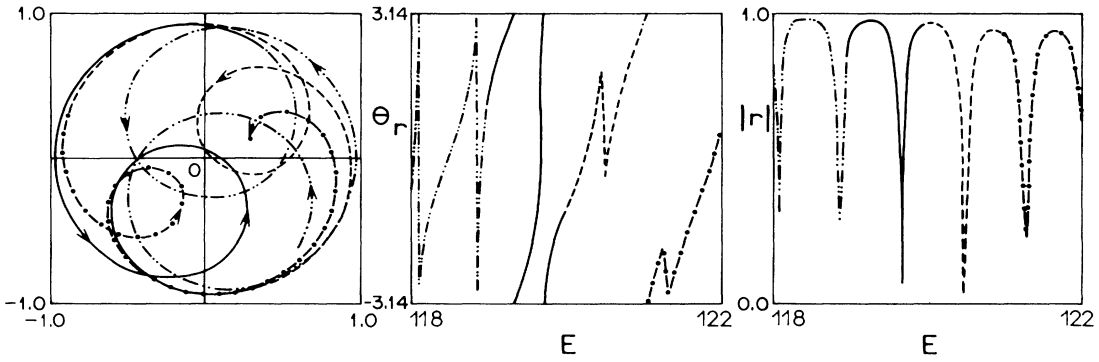

FIG. 7. Same type of data as in Fig. 6 but for a larger energy range. In this case $W=0$, $F=0.8$, $N=100$, and $a=1$. The different marks in the figures correspond to the different energy ranges covered. The figure shows resonances and advanced resonances. Notice the complexity of the curves.

maxima and the HWHM for the different cases, together with their variances, are given in Table I. The results are obtained from resonance averages which had typically 30 resonances. The results presented in Table I correlate well with the Wannier prediction.

Contrary to what happens in the periodic case with $F=0$, the maxima of T are not always one. Also, the HWHM of T is significantly larger in magnitude than the HWHM of $\delta'(E)$. To further understand the properties of T, Fig. 5 shows the behavior of $\theta_r'(E)$, for the parameters used in Fig. 3. The extrema of $\theta_r'(E)$ correspond, almost exactly, to the location of the maxima of T. For instance, the location of the resonance at $E=98.889\,387$ obtained from T, corresponds to the maximum of $\theta_r'(E)$ at $E=98.889\,552$. The agreement between the two numbers covers typically 5 orders of magnitude. In contrast to the behavior of $\delta'(E_n)$ for $E \leq FL$, $\theta_r'(E_n)$ can have not just maxima but also minima as a function of E. This can be understood from looking at r in the complex plane. In Fig. 6, Im(r) versus Re(r), $\theta_r(E)$, and $|r|$ are plotted as E changes for the cases (a) $F=0$, $W=0$, (b) $F=0$, $W\neq 0$, (c) $F\neq 0$, $W=0$, and (d) $F\neq 0$, $W\neq 0$. The first thing to notice is that in the periodic case all the resonances pass through zero, and the angular velocity $\theta_r'(E)$ is always increasing and the change of $\theta_r'(E)$ at resonance is sharp. When $W\neq 0$, there are values of E for which $\theta_r'(E)$ is large but negative, as seen in Fig. 6(b). Also, when $\theta_r'(E)$ is positive, the resonances are not as sharp. For $F\neq 0$, it is seen that as $\theta_r(E)$ approaches zero, the magnitude of r is not always zero at resonance. The magnitude of $\theta_r'(E)$ is an extremum when the magnitude of r reaches its minimum value. When $\theta_r'(E)$ is positive, the phase grows rapidly when the orbit is closest to the origin, and when it is negative it has an abrupt decrease [see Fig. 6(c)]. In the former case, if Wigner's relation between $\theta_r'(E)$ and the time delay is assumed, the value of $\theta_r'(E)$ gives the time the incident wave spends inside the scattering region before it comes out, whereas $\theta_r'(E)<0$ means that the wave in fact moves faster inside the scattering region than in free space.[24] The number of advanced states is smaller than those for which $\theta_r'(E)>0$, though. In Fig. 6(d) the same energy range as in Fig. 6(c) is considered but with $W=0.1$. There it is seen that the disorder modifies the sharpness of the resonances. Finally in Fig. 7 a larger region of energy is shown where maxima and minima in $\theta_r'(E)$ appear as E is changed. The resonances thus correspond to the points in the orbits of Re(r) versus Im(r) closest to the origin, and depending on the sign of the angular velocity at that point the resonance represents a retarded or an advanced scattered wave. In the curves of T versus E, it is seen that each one of the SLR's can be separated from the others and can be approximated by a Breit-Wigner-type form with maxima and HWHM which are weakly dependent on E. Thus, for the nth resonance within a given set of SLR's, T can be approximated by

$$T_n \sim \frac{A_n(\Gamma_n/2)^2}{(E-E_n)^2+(\Gamma_n/2)^2}\ , \tag{19}$$

where A_n is the amplitude characteristic of the nth resonance, and Γ_n and E_n correspond to the HWHM of T and the location of its nth maxima.

Figure 8 shows the behavior of the HWHM of T as a

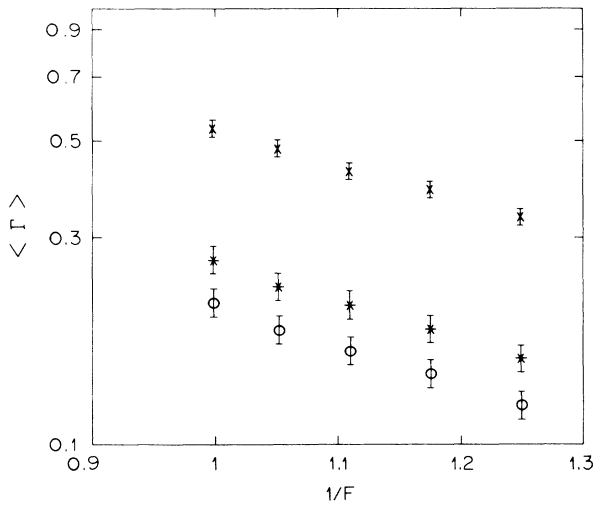

FIG. 8. The half width at half maxima (HWHM), or Γ, of T as a function of $1/F$ shown in a semilogarithmic scale. The parameters used are $a=1$, $N=100$, and $W=0.0$. The curves correspond to the value for V_0 of $V_0=10$ ($\times$), $V_0=20$ ($*$), and $V_0=100$ ($\circ$).

TABLE II. Parameters in Eq. (20) for $V_0=100$, 20, and 10 periodic and disordered cases.

	$W=0$		$W=1$	
V_0	A	B	A	B
100	1.8384	2.1656	1.7864	2.1388
20	2.1282	2.0826	2.0674	2.0095
10	3.4507	1.8879	2.8922	1.5894

function of F, for different heights of the potential V_0. To obtain these results, for each value of F a minimum set of resonances was identified for equivalent energy ranges. The results can be expressed approximately as

$$\Gamma_n(F)=A(V_0)e^{-B(V_0)/F} . \quad (20)$$

The specific values for the constants B and A are given in Table II. This Zener-transmission-type result is very important since from a small change in F the HWHM can go from infinitesimally small to having a finite observable width.

Figure 9, shows the results of Γ as a function of the length of the sample L, for different potentials. These results were obtained changing the zeroth of energy to the top of the ramp since, as L grows, for a given energy range, the number of visible SLR's decreases when the zeroth of energy is at the bottom of the ramp, whereas if $E=0$ at the top the number of resonances can be kept fixed. It is seen that the HWHM is essentially L independent, at least in the range of L's considered, including the fluctuations about its mean value. Similar results were obtained for $\langle \Delta E \rangle$.

The results from Figs. 8 and 9 show that the HWHM of the resonances increases as V_0 decreases. This is intuitively clear from the quantum-mechanical point of view, since the scattering from potentials with smaller height is weaker, and thus the lifetime of the states inside the sample is shorter. In Fig. 10 the behavior for the resistance, as defined in Eq. (17), is presented for the parameter values given in the caption.

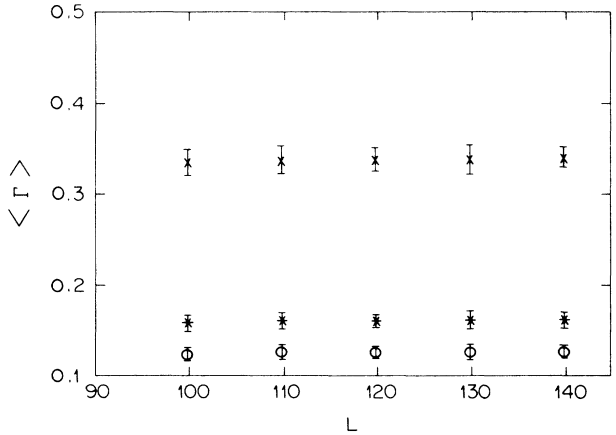

FIG. 9. Γ as a function of the length of the chain L for the different values of V_0, with the same values and notation as in Fig. 8, with $F=0.8$.

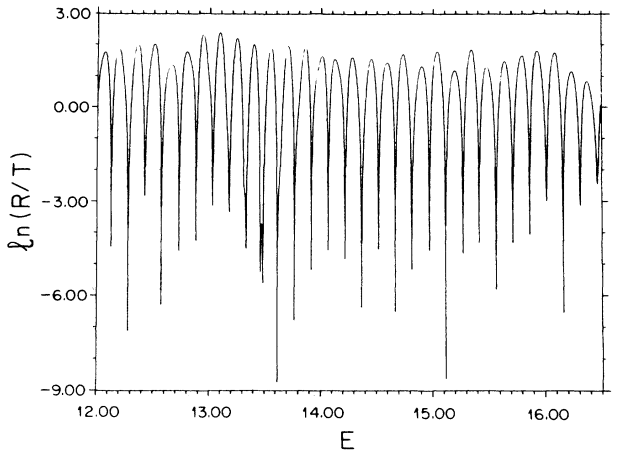

FIG. 10. The logarithm of the resistance as defined in Eq. (3) for the parameters $a=6$, $W=0$, $N=45$, and $F=0.0125$, in a region where the SLR's are clearly visible.

B. SLR's in disordered systems

In this subsection the effects of disorder on the properties of the SLR's will be discussed. The first question to be answered is if the SLR's exist in disordered samples, since the usual proof of the existence of SLR's in periodic systems seems to depend in an essential way on the translational invariance of the potential. Also, since the localization properties of disordered systems in a field depend explicitly on the type of potential present in the sample, the properties of the SLR's as a function of the potential should be addressed.

In Fig. 11(a) and 11(b), $\delta'(E)$ is given as a function of energy for the parameter values given in Fig. 3, but with the potential obtained from the rule defined in Eq. (2) with $W=2$, and $E \leq FL$. When compared to the results of Fig. 3, it is clear that the SLR's are significantly perturbed for this amount of disorder. The two SLR's that are observed in the periodic case, Fig. 3, are no longer clearly distinguishable. Of course, if the amount of disorder is decreased the SLR's become visible again. These results, when compared with the ones given in the periodic case, indicate that the SLR's for $E \leq FL$ are not stable against the addition of relatively small amounts of disorder. For smaller amounts of disorder the SLR's are visible again, however, but there are some changes that depend on the specific distribution of potentials in the sample.

The situation is however different for $E \geq FL$, for the same amount of disorder. In Fig. 12 we present the transmission coefficient as a function of E for the same parameter values as in Fig. 11. In this case the SLR's are clearly seen, with the widths, heights and separation distances changing slightly with W. The corresponding result for the logarithm of the resistance in the disordered case for the parameters used in Fig. 10 is given in Fig. 13.

To carry out a systematic analysis of the properties of the SLR's in disordered systems, we need to calculate en-

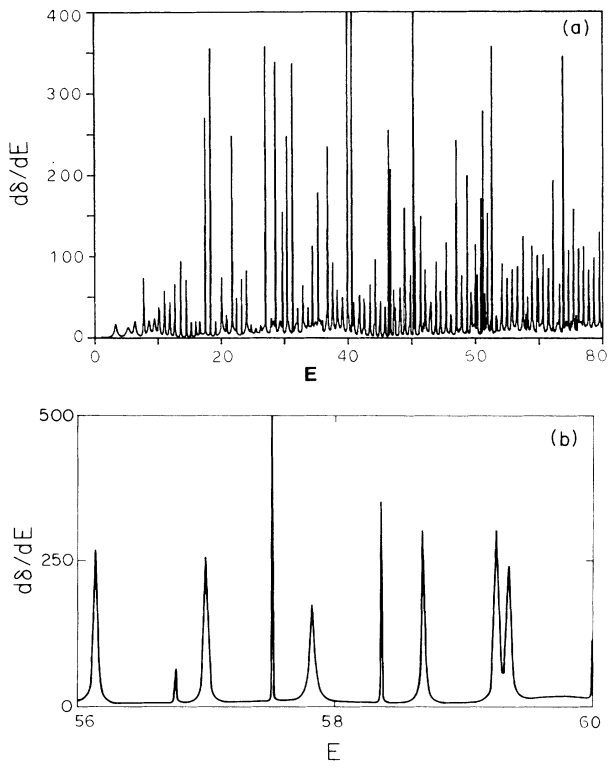

FIG. 11. Plots of $\delta'(E)$ for two energy scales for the same parameters as in Figs. 3(a) and 3(b), but with $W=2$.

semble and resonance averaged quantities. We start by numerically generating a set of chains with potentials chosen from Eq. (3). Typically the ensembles had 20 members leading to good statistics. The expressions for the mean values, denoted by $\langle\ \rangle$, and their corresponding variances of the quantities of interest are obtained as follows. Call Y the quantity to be averaged, then the mean value is given by,

$$\langle Y\rangle=\frac{1}{Mn}\sum_{i,j}Y_{ij}\ ,$$

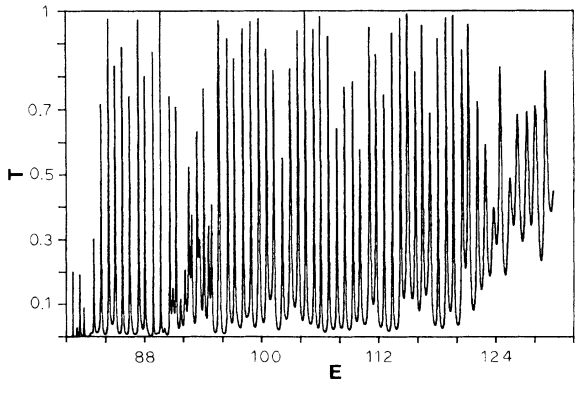

FIG. 12. The transmission coefficient T as a function of E, for the same parameter values as in Fig. 11 with $FL\leq E$.

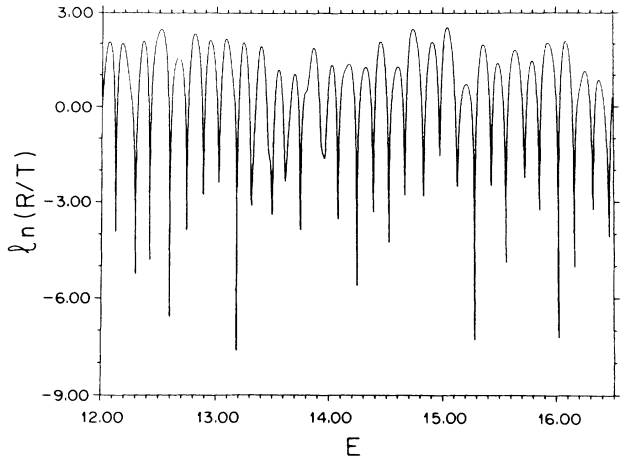

FIG. 13. The logarithm of the resistance with parameters as in Fig. 10 in the disordered case with $W=2$.

where n is the number of resonances in the ith sample, and j runs from $1,\ldots,M$, the number of samples. The variance is obtained from,

$$\sigma_Y^2=\frac{1}{Mn}\sum_i(\langle Y_i\rangle-\langle Y\rangle)^2\ .$$

Here, $\langle Y_i\rangle$ is the mean value of Y for the ith sample.

The behavior of the mean separation distance between resonances grows linearly with W with a very small slope, indicating that the Wannier states are still visible on the average. However, the fluctuations about the mean value increase significantly as W increases (see Fig. 14). In fact, as W grows the SLR's tend to disappear since the localization of the wave function induced by disorder starts to dominate the localization produced by the field. This result will be discussed further in the last section. $\langle\Gamma\rangle$ as a function of W grows quadratically, but with fluctuations that are significantly smaller than in the case of $\langle\Delta E\rangle$.

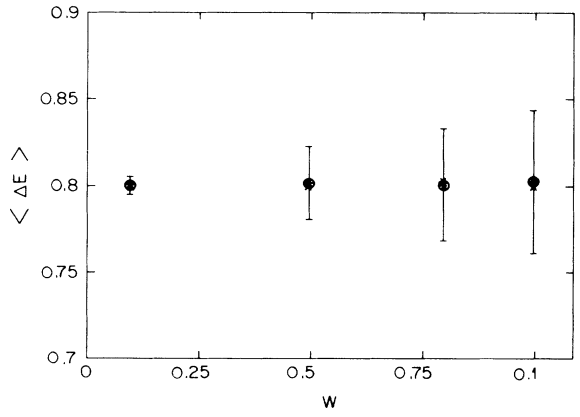

FIG. 14. Resonance and ensemble averaged $\langle\Delta(E)\rangle$, as a function of W, for $N=100$, $a=1$, and $F=0.8$. Notice the increase of the fluctuations about the mean value as W increases. The calculation was done for the three different values of V_0 used in Fig. 8. with the same notation.

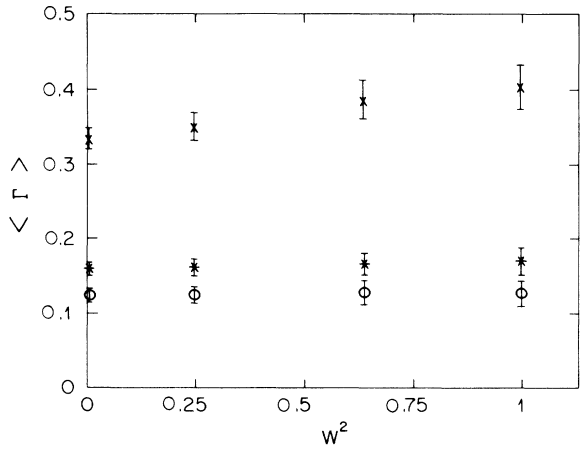

FIG. 15. The HWHM of the transmission coefficient Γ as a function of W^2 shown in this figure for the different values of V_0 as in Fig. 14 and with the same parameters for N, a, and F.

In Fig. 15 the averaged HWHM as a function of W^2 is shown. The slopes in these curves, m, for the different cases are $m(V_0=100)=0.002\,418$, $m(V_0=20)=0.114\,38$, and $m(V_0=10)=0.755\,40$, the largest being the $V_0=10$ case.

The averaged $\langle\Gamma\rangle$ as a function of F is shown in Fig. 16, with $W=1$. As in the periodic case the Zener-tunneling-type result given in Eq. (20) remains. The specific values for B and A are given in Table II. There is a small but explicit quantitative change in the results. The quantitative differences arise from an increase in the fluctuations about the mean values as well as a decrease of the lifetime of the SLR's in the case $V_0=10$. Finally, the dependence of the HWHM with respect to L is given in Fig. 17. As in the case of $W=0$ the mean value of $\langle\Gamma\rangle$ remains essentially constant for the range of L's considered. Quantitatively, the fluctuations about the mean values increase and the lifetime of the $V_0=10$ case is significantly reduced by disorder.

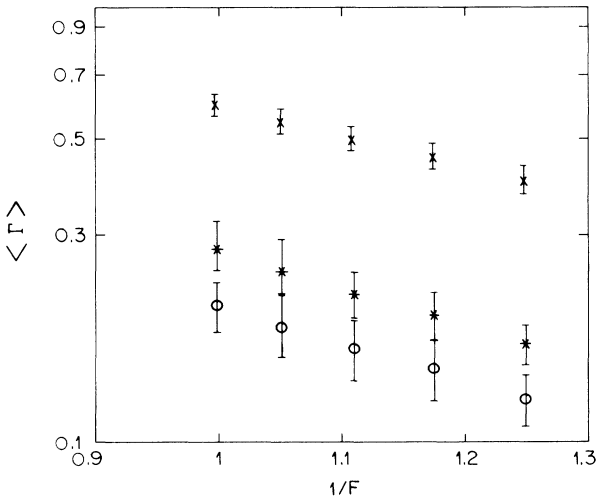

FIG. 16. Resonance and ensemble average $\langle\Gamma\rangle$ as a function of $1/F$ with $W=1$, for the same parameter values as in Fig. 15 with the same notation.

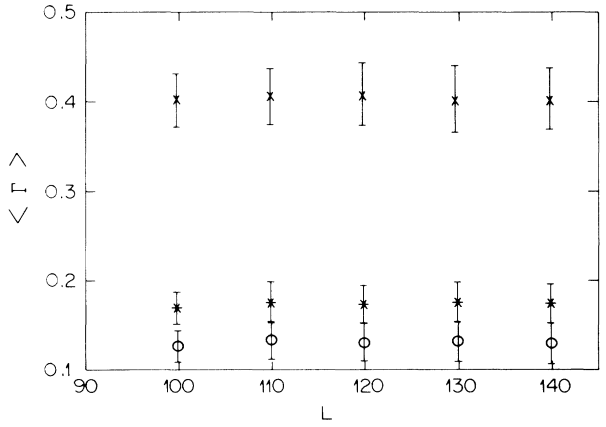

FIG. 17. The same as in Fig. 9. for the same parameters except that $W=1$.

From the results presented in this subsection, we conclude that if the disorder is not too big the SLR's will appear in the electronic spectrum. The specific statistical properties of the SLR's will depend quantitatively on the properties of the potential but not qualitatively.

IV. LOW-TEMPERATURE EFFECTS ON SLR's

One of the most important factors that may determine the feasibility of seeing the SLR's experimentally is the temperature. Since the values of the fields necessary to clearly see the SLR's are relatively large, the interaction of the electrons with the phonons becomes important. Also, of relevance are the thermal population effects related to the distribution of energies of the electrons at finite temperature. The phonon effects can be neglected in the limit of sample size smaller than the inelastic mean free path l_{in}. This condition may not be easy to fulfill experimentally, however. In this regime, only the thermal population effects are important, and we consider these effects in this section. In fact, within the formalism used in this paper, the contribution of the phonons is not easily incorporated, although phenomenologically it would be possible. In Sec. IV A the periodic case is discussed and in Sec. IV B the disordered case is considered briefly.

A. Periodic case

In the $F=0$ disordered case the thermal population effects have been discussed extensively.[25] Here we extend these analyses to the $F\neq 0$ case. Since we do not have a Landauer-type formula for arbitrary F at finite temperature, we concentrate on calculating the thermal average of the transmission coefficient, which is always well defined. The transmission coefficient as a function of the chemical potential μ, and temperature τ, is given as[17]

$$T(\mu,\tau)=-\int \left|\frac{\partial f(\mu,E)}{\partial E}\right| T(E)dE \ . \tag{21}$$

Here $f(\mu,\tau)$ is the Fermi-Dirac distribution function given as,

$$f(\mu,\tau)^{-1}=(e^{(E-\mu)/k_B\tau}+1)\ ,$$

and k_B is the Boltzmann constant. Since $-\partial f(\mu,E)/\partial E$ is a strongly peaked function of E, the integral will be essentially zero outside of an interval of width $k_B\tau$. Thus, to calculate $T(\mu,\tau)$ for a given τ, first a SLR is found at $\tau=0$. The temperature range is chosen such that $k_B\tau<\langle\Gamma\rangle$. For a given energy in the range where there are SLR's, typically we chose an interval of width $5k_B\tau$, around the chosen energy E. The calculation of $T(E)$ is carried out for at least 10 different values, and the integral is then evaluated numerically. Each point in the plots shown in Fig. 18 is obtained this way. The values of the temperatures considered are $\tau=0.0001$, 0.001, and 0.01. The other parameter values are given in the caption. Notice that the effect of increasing temperature is to reduce the average height of the resonances. However, the decrease is not uniform as μ changes. If we assume that each one of the SLR's can be approximated by a Breit-Wigner form, as given in Eq. (19), the contribution to $T(\mu,\tau)$ around the nth resonance can be written as

$$T_n(\mu,\tau)\sim\int\left|\frac{\partial f(\mu,E)}{\partial E}\right|T(E)\frac{(\Gamma_n/2)^2}{(E-E_n)^2+(\Gamma_n/2)^2}dE\ . \tag{22}$$

At sufficiently low temperatures we can approximate $\partial f(\mu,E)/\partial E\sim-(1/\tau)e^{-|E-\mu|/k_B\tau}$. When τ is very low, the main contribution to $T_n(\mu,\tau)$ comes from points around the resonance at E_n, such that the integral can be evaluated asymptotically giving,

$$T_n(\mu,\tau)\sim\frac{1}{\tau}e^{-|E_n-\mu|/k_B\tau}\left[T(E_n)\sin(\Gamma_n\beta)-\frac{\Gamma}{2}T'(E_n)\cos(\Gamma_n\beta)\right]\ . \tag{23}$$

where $\beta=1/k_B\tau$, Γ_n has been assumed small, and $T(E_n),T_n'(E_n)$, are the transmission coefficient at reso-

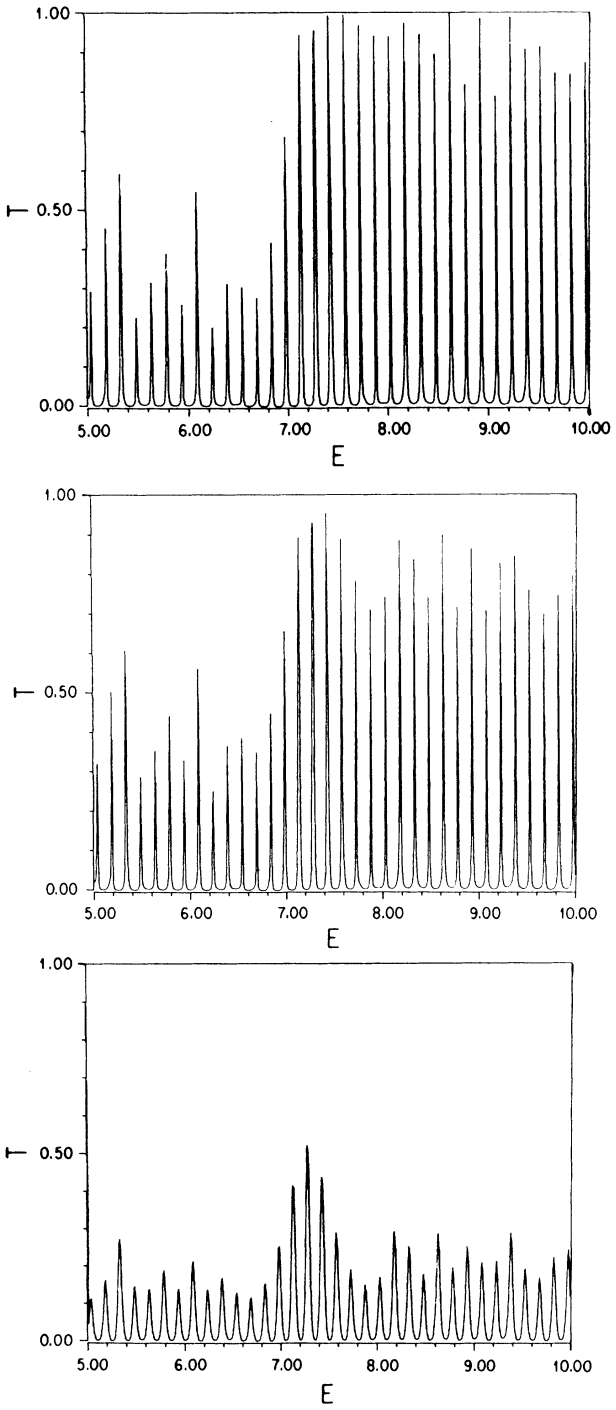

FIG. 18. Thermal population effects of SLR's as seen in terms of $T(E)$. The parameters used are $N=45$, $F=0.025$, $W=0$, $V_0=100$, and $a=6$. Top figure, $\tau=0.0001$, middle, $\tau=0.001$, and bottom, $\tau=0.01$.

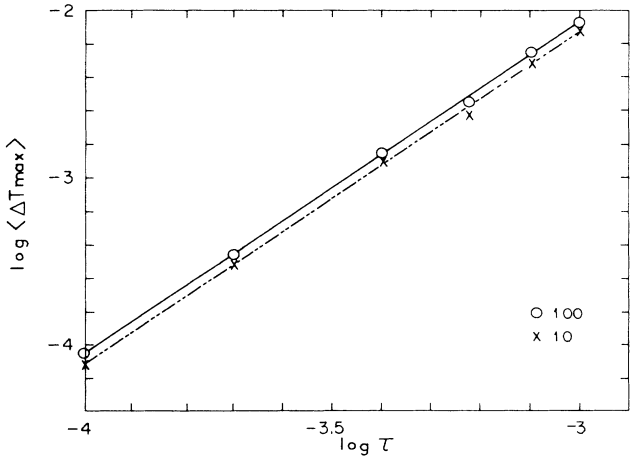

FIG. 19. Log-log plot of the rate of change of $T_{\max}$ as a function of τ. The slope is almost exactly -2. The parameter values are $N=45$, $F=0.025$, $a=6$, $W=0$, $V_0=100$ (○) and 10 (×).

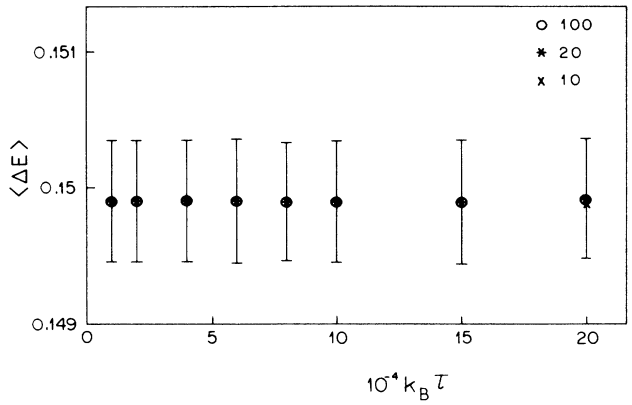

FIG. 20. $\langle \Delta E \rangle$ vs τ for the same parameter values as in Fig. 19 with $V_0=20$ (*).

nance and its corresponding derivative with respect to E. This is a general result for any resonance that can be expressed by a Breit-Wigner form. For the SLR case $E_n = Fna$. Equation (23) makes explicit the fact that different resonances produce different changes in $T_n(\mu,\tau)$. Since we have taken $\Gamma\beta > 1$, the oscillatory behavior of $T_n(\mu,\tau)$ is outside of the range considered in our numerical results. However, from measuring the average rate of change of the maxima of T as a function of τ, the results obtained in Fig. 19 agree with the τ^{-2} prediction of Eq. (23) at resonance for the extreme δ potential and for $V_0=10$.

Figure 20 shows the average separation distance $\langle \Delta E \rangle$ as a function of τ, for a restricted temperature range, for the rectangular potential barriers with heights $V_0=100$, 20, and 10. These results indicate that the mean separation distance between SLR's remains constant as τ increases, and the corresponding fluctuations remain constant as well. In Fig. 21 the corresponding results for the HWHM are given in the same temperature range as in Fig. 20. Notice the scale in the vertical axis of the figure. In contrast to $\langle \Delta E \rangle$, $\langle \Gamma \rangle$ increases slightly as τ increases,

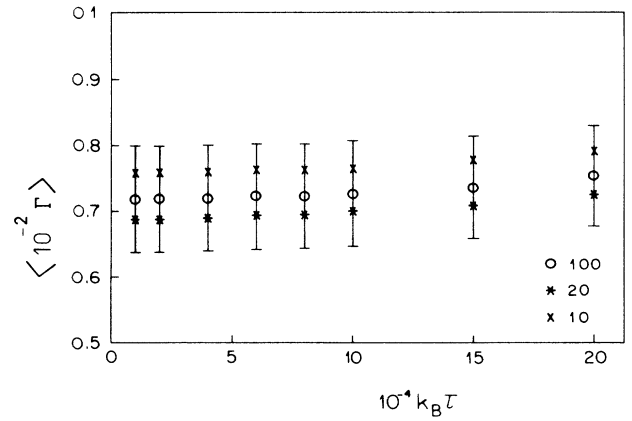

FIG. 21. $\langle \Gamma \rangle \times 10^{-2}$ vs τ. The parameters are equal to those in Fig. 20. Notice that the scale in the vertical axis is multiplied by 10^{-2}.

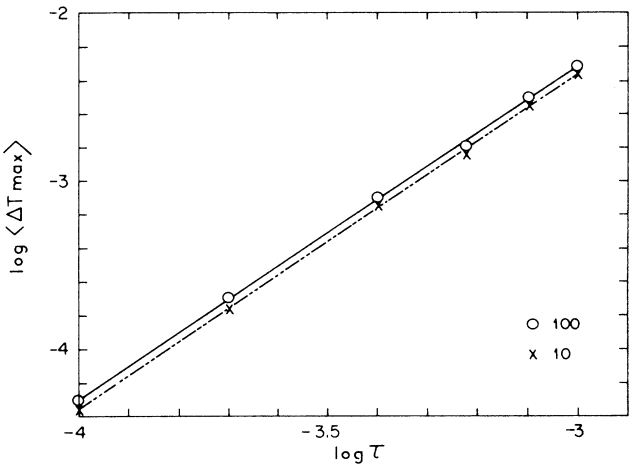

FIG. 22. The same as in Fig. 19 with all the parameters the same but with $W=1$.

in agreement to what is seen visually, that the SLR's become wider as τ increases. The fluctuations of Γ are, however, smaller.

B. Disordered case

In Sec. III it was seen that the SLR's are essentially stable against small amounts of disorder. Therefore we expect that at finite temperatures the results obtained in Sec. IV A should change quantitatively but not qualitatively. In Fig. 22 the average of the rate of change of the maxima of T with respect to τ as a function of τ is shown. The ensemble has 20 samples, and $W=1$. As in the $W=0$ case, the slope of the curves is very close to -2, but the intercept with the vertical axis is different.

Figures 23 and 24 present the results of a resonance and ensemble averaged $\langle \Delta E \rangle$ and $\langle \Gamma \rangle$ as a function of temperature. Again notice the scale in Fig. 24. In both figures it is seen that there is a very small variation of the results as τ changes. However, the fluctuations about the mean values have increased more than threefold as compared to those of Figs. 21 and 22.

In summary, we see that increasing the temperature has

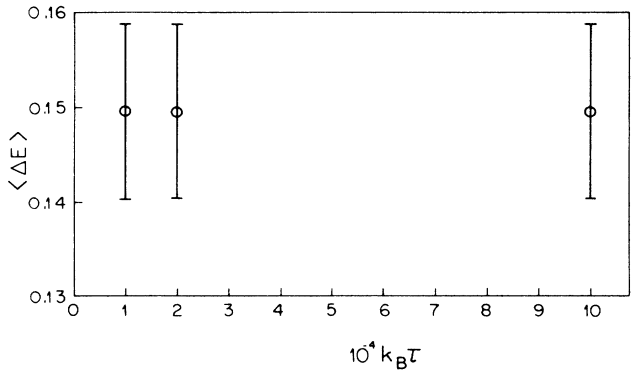

FIG. 23. The same as in Fig. 20 with the same parameters except $W=1$.

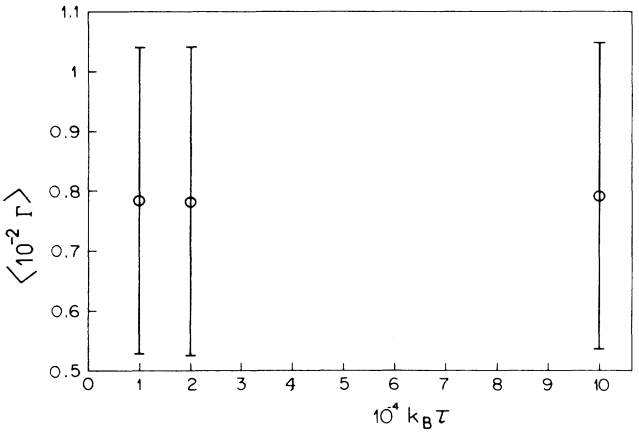

FIG. 24. The same as in Fig. 21 with disorder $W=1$ and all the other parameters the same.

the effect of decreasing the magnitude of the natural linewidth of the SLR's, while the average separation distance between SLR's remains equal to *Fna*. The effect of disorder is that of increasing the fluctuations about the $\tau=0$ results, thus making them harder to see.

V. SUMMARY AND CRITIQUE OF THE RESULTS

In this paper a thorough analysis of the Stark-ladder resonances (SLR's) in one-dimensional periodic and disordered systems has been given. Using different scattering theory criteria, the SLR's have been analyzed as a function of different parameters: the length of the sample L, the magnitude of the field F, the height and width of the potentials V_0 and b, the amount of disorder W, and the temperature τ. Only thermal population effects have been considered. The analysis has been carried out in the regions for which the electron incoming energy E is either smaller than FL or larger. Both regimes are different with respect to their scattering properties. The experimentally relevant regime corresponds to $E \geq FL$. The SLR's were analyzed in both regimes when the potentials were periodic and of different heights. For $E \leq FL$, the phase shifts of the S matrix were analyzed to obtain the properties of the SLR's. Above the barrier (i.e., for $E \geq FL$) the SLR's were analyzed in terms of the maxima of T as a function of E. The half width at half maximum was used to characterize the properties of the SLR's. Each one of the SLR's for $E \geq FL$ can be approximated by a Breit-Wigner-type form. It was found that there is a minimum value of the field above which the SLR's are clearly visible (see also Ref. 6). The properties of the SLR's, above and below the potential produced by the field are different, e.g., for $E \leq FL$ there are two SLR's that are clearly visible, while for $E \geq FL$ there is only one, for the same energy mesh. Also the HWHM of $\delta'(E)$ or of $T(E)$ are different, several orders of magnitude smaller in the former than in the latter. We concentrated mostly in the analyses of the SLR's as seen for $E \geq FL$, which is the regime of experimental interest, and not studied previously. When the temperature is increased, the natural linewidth of the SLR's increases while the maxima of the transmission coefficient decreases essentially as $1/\tau$, for low temperatures.

Adding disorder has the effect of perturbing the properties of the resonances. For small amounts of disorder the SLR's are stable. However, the SLR's for $E \leq FL$ are less stable than the SLR's for $E \geq FL$, for the same amount of disorder. As the disorder increases, the fluctuations about the mean values increase as well. Although the SLR's are clearly visible for each sample with a disordered potential, statistically sound results were obtained from resonance and ensemble averaged quantities. When the disorder is increased significantly, the SLR's essentially disappear.

The results given above can be understood from the following physical reasoning: In the periodic case without a field, an electron with energies within a band can move freely across the sample. When the periodic system is subjected to an electric field, the electron is confined to a region in space of the order of $l_F=E/F$. This confinement is produced by the band edges in the E versus x plot, e.g., the tilted band picture introduced by Zener. The electron is accelerated by the field across the tilted band. When it gets to the ends of the band, the electron is reflected and thus is able to complete closed orbits in momentum space. Quantizing these closed orbits in momentum space *á la* Bohr-Sommerfeld is what produces the Wannier states. However, there is a possibility of tunneling from one of the bands to the others, thus converting the Wannier states into resonances. The time spent by the electron trapped within a band is inversely proportional to $\Gamma_n(F)=Ae^{-B/F}$ [Eq. (20)]. This result implies that changing F slightly produces an exponential change in the time spent by the electron within a band. This exponential behavior of the lifetime is essential to be able to see the SLR's experimentally. When disorder is added to the system a new length becomes important, the localization length $l_{\rm loc}(X)$. When $F\neq 0$, $l_{\rm loc}$ becomes a strong function of $X=FL/E$. The behavior of $l_{\rm loc}(X)/l_{\rm loc}$ $(F=0,E,W)$ depends strongly on the type of potential considered.[10,12,19] The explicit dependence of $l_{\rm loc}$ $(F=0,E,W)$ has been considered in Ref. 19. When the disorder is small $l_{\rm loc} \gg l_F$, the electron is able to complete closed orbits and thus the appearance of SLR. As the electron tunnels to other bands the effects of disorder are felt and the properties of the SLR's are qualitatively modified. As the disorder is increased, and $l_{\rm loc}$ becomes comparable to l_F the electron is not able to complete many closed orbits and the SLR's essentially disappear.

In the disordered case, when the SLR's are clearly visible, the HWHM is stable as L increases, provided the field $F<F_c$. In fact, in the disordered δ-potential case, in the regime $X>1$, the power law decay of T helps stabilize the HWHM of the SLR's.[18,19] A qualitatively similar effect occurs when the potential V_0 is of finite height. The magnitude of the height of V_0 has an important quantitative effect in the HWHM. Thus, Γ is larger for smaller V_0's thus making the SLR's more likely to be seen when the potential is of finite height.[12]

We now discuss the limitations of the model studied in this paper as compared to real experimental conditions. It is clear that temperature will play a significant role in the

possible observation of SLR's experimentally. Since the electric fields at which the SLR's are clearly distinguishable are relatively high, the coupling of the lattice to the electronic SLR states will be of relevance, and could even destroy the SLR's. However, it is not clear as to how to include the phonon effects in a detailed theory at the same level of rigor as the analysis of SLR's presented here. The results of Secs. III and IV will remain valid if the inelastic mean free path l_{in} is much larger than the dimensions of the sample L. Of course, the l_{in} may be also a function of F. In the presence of a field F there are at least four lengths that are important: l_{in}, l_F, l_{loc}, and l_{el} the elastic mean free path, which is sometimes related to l_{loc}. Thus, experimental conditions have to be produced such that passing a current of the order needed to see the SLR's does not melt the wire before the resonances are seen.

As mentioned above, in order to be able to see the SLR's experimentally, it is necessary that $l_{in} \geq L$ such that the phonon effects do not destroy the phase coherence needed to have the SLR's clearly defined. Experimentally this implies ultralow temperatures and ultrasmall wires.

The length l_F is important because it defines the lengths for which the electronic trajectories are localized by the field, and thus the appearance of SLR's. Also, l_F separates the regions for which localization effects are important from those from which the field is important. We have seen that the thermal averaging as defined in Sec. IV does not destroy the SLR's and only modifies its main features. Of course, the finite τ analysis has been done in analogy with the small field calculations,[25] without having a connection with an experimentally measurable quantity, although the average of T as given in Eq. (21) is always well defined.

Another experimental shortcoming of the model studied here is that electron-electron interactions have been neglected. Resonance tunneling, when there is screening has not been studied in detail as yet. Thus, the calculations presented here are more appropriate for a semiconductor than for a metal.

One more aspect of the model studied here is that it is one dimensional. In a recent paper the density of states of a one-, two-, and three-dimensional periodic lattice in a field F has been calculated.[26] There it was found that SLR's are sharply defined only in one dimension. Thus, the likelihood of seeing the SLR's is higher in one dimension than in higher dimensions. In this respect, it is possible that the SLR's could also be seen in superlattices, since these systems can be approximated as one-dimensional. The bandwidth can be tailored at will, and thus the dissipation effects can be minimized, as well as the magnitude of F necessary to see the SLR's can be reduced.[27]

ACKNOWLEDGMENTS

Two of us (E.C. and G.M.) thank the hospitality of Northeastern University (Boston, MA), where most of this work was carried out. They also thank the National University of Mexico and the National Council for Science and Technology of Mexico [Consejo Nacional de Ciencia y Tecnologia (CONACyT)] for financial support. One of us (E.C.) also thanks the The American Physical Society (APS) for partial support. One of us (J.J.) thanks the Physics Institute of the University of Mexico for its hospitality while this work was completed. This work has been supported in part by the National Science Foundation Grant No. DMR-86-40360.

*Present address: Institute Max von Laue—Paul Langevin, Avenue des Martyrs, Boîte Postale 156X, 38042 Grenoble, Cédex, France. Permanent address: Physics Department, Northeastern University, Boston, MA 02115.

[1]I. M. Lifshitz and V. Ya. Kirpichenkov, Zh. Eksp. Teor. Fiz. **77**, 989 (1979) [Sov. Phys.—JETP **50**, 499 (1979)].

[2]M. Ya. Azbel, Phys. Rev. B **28**, 4106 (1983); M. Ya. Azbel and P. Soven, *ibid.* **27**, 831 (1983).

[3]R. E. Webb, A. Hartstein, J. J. Wainer, and A. B. Fowler, Phys. Rev. Lett. **54**, 1577 (1985); W. J. Skocpol, L. D. Jackel, R. E. Howard, and C. A. Fetter, *ibid.* **49**, 951 (1982); R. F. Kwasnick, M. A. Kastner, J. Melnagailis, and P. A. Lee, *ibid.* **52**, 224 (1984).

[4]A. B. Fowler, G. L. Timp, J. J. Wainer, and R. A. Webb, Phys. Rev. Lett. **57**, 138 (1986).

[5]G. H. Wannier, Phys. Rev. **117**, 432 (1960); Rev. Mod. Phys. **34**, 645 (1962).

[6]F. Bentosela, V. Grecchi, and F. Zironi, J. Phys. C **15**, 7119 (1982).

[7]L. M. Lambert, J. Phys. Chem. Solids **26**, 1409 (1965); Phys. Rev. **138**, A1569 (1965); R. W. Koss and L. M. Lambert, Phys. Rev. B **5**, 1479 (1972).

[8]V. N. Prigodin, Zh. Eksp. Teor. Fiz. **79**, 2338 (1980) [Sov. Phys.—JETP **52**, 1185 (1980)].

[9]J. Flores, J. V. José, and G. Monsiváis, J. Phys. C **16**, L103 (1983).

[10]C. M. Soukoulis, J. V. José, E. N. Economou, and P. Sheng, Phys. Rev. Lett. **50**, 764 (1983).

[11]F. Delyon, B. Simon, and B. Soulliard, Phys. Rev. Lett. **52**, 2187 (1984).

[12]E. Cota, J. V. José, and M. Ya. Azbel, Phys. Rev. B **32**, 6157 (1985).

[13]T. Kirkpatrick, Phys. Rev. B **33**, 780 (1986).

[14]J. Flores, P. A. Mello, and G. Monsiváis, Phys. Rev. B **35**, 2114 (1987).

[15]P. Erdös, and R. C. Herndon, Adv. Phys. **31**, 65 (1982).

[16]J. R. Banavar and D. D. Coon, Phys. Rev. B **17**, 3744 (1978).

[17]M. Ya. Azbel, A. Hartstein, and D. P. DiVincenzo, Phys. Rev. Lett. **52**, 1641 (1984); D. P. DiVincenzo and M. Ya. Azbel, *ibid.* **50**, 2102 (1983).

[18]J. V. José, G. Monsiváis, and J. Flores, Phys. Rev. B **31**, 6906 (1985).

[19]For a complementary analysis, see F. Bentosela, V. Grecchi, and F. Zironi, Phys. Rev. B **31**, 6909 (1985).

[20]R. G. Newton, *Scattering Theory of Particles and Waves,* 2nd. ed. (Springer-Verlag, Berlin, 1982).

[21]J. Bellisard, A. Formoso, R. Lima, and D. Testard, Phys. Rev. B **26**, 3024 (1982).
[22]J. Zak, in *Solid State Physics,* edited by H. Ehrenreich *et al.* (Academic, New York, 1972), Vol. 27, p. 1.
[23]R. Landauer, Philos. Mag. **21**, 863 (1970).
[24]K. W. McVoy, *Fundamentals in Nuclear Theory* (International Atomic Energy Agency, Vienna, 1967).
[25]H. L. Engquist and P. W. Anderson, Phys. Rev. **24**, 1151 (1981); M. Ya. Azbel, A. Hartstein, and D. P. DiVincenzo, Phys. Rev. Lett. **53**, 2042 (1984); **53**, 1641 (1984).
[26]L. Pacheco and F. Claro (unpublished).
[27]J. E. Avron, Ann. Phys. **143**, 33 (1982).